Image Denoising Games

Yan Chen, *Member, IEEE,* and K. J. Ray Liu, *Fellow, IEEE*

***Abstract*—Based on the observation that every small window in a natural image has many similar windows in the same image, the nonlocal denoising methods perform denoising by weighted averaging all the pixels in a nonlocal window and have achieved very promising denoising results. However, the use of fixed parameters greatly limits the denoising performance. Therefore, an important issue in pixel-domain image denoising algorithms is how to adaptively choose optimal parameters. While the Stein's principle is shown to be able to estimate the true mean square error (MSE) for determining the optimal parameters, there exists a tradeoff between the accuracy of the estimate and the minimum of the true MSE. In this paper, we study the impact of such a tradeoff and formulate the image denoising problem as a coalition formation game. In this game, every pixel/block is treated as a player, who tries to seek partners to form a coalition to achieve better denoising results. By forming a coalition, every player in the coalition can obtain certain gains by improving the accuracy of the Stein's estimate, while incurring some costs by increasing the minimum of the true MSE. Moreover, we show that the traditional approaches using same parameters for the whole image are special cases of the proposed game theoretic framework by choosing the utility function without a cost term. Finally, experimental results demonstrate the efficiency and effectiveness of the proposed game theoretic method.**

***Index Terms*—Coalition formation, game theory, image denoising, Stein's principle.**

I. Introduction

During the processes of being captured, digitized, recorded, and transmitted, an image is usually distorted and noisy. Such a noisy image is visually annoying and often not suited to further perform tasks such as segmentation, recognition and compression. Therefore, image denoising is a very important issue to reconstruct a good estimate of the original image from the noisy observations.

Many approaches have been proposed in the literature to reconstruct the original image by exploiting the inherently spatial correlation. By assuming that the image locally satisfies a stationary Gaussian process, Woods and Radewan [1] propose to estimate the original image from the noisy image using Kalman filter while Jin *et al.* [2] propose to use adaptive Wiener filter. In both approaches, the first-order and second-order statistics used in the filters are calculated based on the noisy samples within a local window. In [3]–[5], the authors propose to use bilateral filtering over the local neighborhood samples, where the weights of the bilateral filters are computed based on the intensity and radiometric distances between the center sample and the neighboring samples. Another class of locally adaptive image denoising approaches are derived by considering image processing as a variational problem where the restored image is computed by minimizing a carefully designed energy function [6]–[8]. Typically, such energy functions consist of a fidelity term that is determined by the difference between the reconstructed image and the noisy image, and a regularization penalty term that is determined by the image prior.

To further exploit the spatial correlation, Buades *et al.* [9] proposed to average, in a weighted manner, all the pixels in a nonlocal window instead of only involving the locally neighboring pixels, where the weights are determined by the differences between the region centered by the target pixel and the regions centered by the candidate pixels. Since the weights are not determined by the radiometric (physical) distance, similar pixels that are far away from the target pixel can still be awarded large weights. In such a way, the denoising performance is greatly improved. Several extensions of the nonlocal approach are also proposed [10]–[12].

Besides the pixel-domain approaches, transform-domain approaches are also investigated [13]–[16]. The transform-domain approaches are mainly based on the assumption that the original signal can be well-approximated by a linear combination of few basis, i.e., the original signal is sparse in the transform-domain. In such a case, the original signal can be well estimated by preserving the few high-magnitude transform coefficients that convey mostly the energy of the original signal and discarding the rest which are mainly introduced by the noise. Therefore, one important issue in the transform-domain approaches is how to threshold the transform coefficients. Many threshold rules have been proposed from different speculations [13], [17], and [18]. A combination of the nonlocal and transform-domain thresholding ideas is proposed in [19]. The basic idea is to first group similar 2-D image blocks into 3-D data arrays, then perform 3-D wavelet transform, and finally shrinkage the transform spectrum. A similar idea is proposed to combine non-local with sparse coding as well as dictionary learning [20], [21] .

Most of the existing schemes focus on how to choose good weights to achieve better reconstructions by using the same parameters for the whole image. However, how to adaptively choose optimal parameters can be very important since using the same parameters for the whole image may cause severe artifacts such as fake edge artifacts and over-smooth artifacts. The theoretical and empirical study in [22],

Manuscript received September 24, 2012; revised February 2, 2013; accepted March 21, 2013. Date of publication March 28, 2013; date of current version September 28, 2013. This paper was recommended by Associate Editor R. Lukac.

The authors are with the Department of Electrical and Computer Engineering, University of Maryland, College Park, MD 20742 USA (e-mail: yan@umd.edu; kjrliu@umd.edu).

Color versions of one or more of the figures in this paper are available online at http://ieeexplore.ieee.org.

Digital Object Identifier 10.1109/TCSVT.2013.2255433

[23] reveals that existing denoising algorithms are close to the optimal performance with fixed patch size, and suggests to use novel adaptive variable-sized patch schemes to improve the denoising performance of existing algorithms. Due to the absence of the original image, the Stein's principle [24] is used to estimate the true MSE for determining the optimal parameters. With such a principle, the parameters can be adjusted to achieve better denoising performance, such as the nonlocal based methods [25], [26], wavelet thresholding based methods [27]–[29], and general numerical procedure for denoising [30]. Nevertheless, we find that there exists a tradeoff between the accuracy of the estimate and the minimum of the true MSE. In this paper, we study the impact of this tradeoff and formulate the image denoising problem as a coalition formation game.[1] In this game, every pixel/block is treated as a player, who tries to seek partners to form a coalition to improve the accuracy of the Stein's estimate while incurring a cost of increasing the minimum of the true MSE. Since finding the optimal coalition structures is NP-hard, we propose a heuristically distributed algorithm in solving the coalition formation game. We also show that the traditional approaches that use the same parameters for the whole image are special cases of the proposed game theoretic framework by choosing the utility function without a cost term. Finally, experimental results are shown to demonstrate the efficiency and effectiveness of the proposed method. Note that the proposed game is also applicable to other scenarios besides the pixel-domain denoising method as long as: 1) there exists some locally adaptive parameters to be estimated and; 2) the estimation accuracy will be improved when more samples are involved in the estimate process.

The rest of this paper is organized as follows. In Section II, we give a brief description of the system model and the coalition formation game. Then, we discuss in details the proposed game theoretic denoising framework in Section III, including the confidence and distortion tradeoff of the Stein's unbiased risk estimate, the game theoretic formulation and the corresponding solution. In Section IV, we show the relationship between the proposed game-theoretic framework and the traditional approaches that use the same parameters for the whole image. Finally, we illustrate the experimental results on real images in Section V and draw conclusions in Section VI.

II. System Model and Coalition Formation Game

A. System Model

In this paper, we consider the problem of restoring images degraded by additive white Gaussian noise. The degraded process can be modelled as

$$I^n(\mathbf{k}) = I(\mathbf{k}) + n(\mathbf{k}) \tag{1}$$

where I is the original image, I^n is the noisy observation of the image, and n is the additive Gaussian noise with zero mean and σ^2 noise variance. The $\mathbf{k} = (k_1, k_2)$ is the coordinate of a pixel. The problem is to find an estimate $\hat{I}$ of the original image based on the noisy observation I^n.

[1]Part of this paper has been presented in [31].

It is well known that the image denoising problem is ill posed. To reconstruct the original image from the noisy observation, we need to use some prior information such as the correlations among spatial neighboring pixels. In this paper, we focus on the spatially adaptive linear filtering approach. For the pixel located at $\mathbf{k}$, we find the estimate $\hat{I}(\mathbf{k})$ using the weighted average of the spatially neighboring pixels, that is

$$\hat{I}(\mathbf{k}) = \frac{\sum_{\mathbf{l}\in S(\mathbf{k})} w_{\mathbf{k},\mathbf{l}} I^n(\mathbf{l})}{\sum_{\mathbf{l}\in S(\mathbf{k})} w_{\mathbf{k},\mathbf{l}}} \tag{2}$$

where $S(\mathbf{k})$ is the candidate set that contains the spatially neighboring pixels for $\mathbf{k}$, and $w_{\mathbf{k},\mathbf{l}}$ is the weight for pixel $I^n(\mathbf{l})$.

B. The Coalition Formation Game

Game theory is a mathematical tool that analyzes the strategic interactions among multiple decision makers. A game is mainly composed by three components:

1) a finite set of players, denoted by $u_1, u_2, ..., u_N$;
2) a set of actions, denoted by A_i, for each player u_i;
3) payoff/utility function, denoted by U_i, which measures the outcome for player u_i determined by the actions of all players.

A coalition formation game is a game where the players seek to form cooperative groups, i.e., coalitions, to strengthen their positions in the game. The players' actions in the coalition formation game are whom to cooperate with, i.e., which players to form coalitions with. The payoff/utility function in the coalition formation game is defined over coalitions, called coalition value. The coalition value, which quantifies the worth of a coalition, is mainly determined by two terms: the gain and the cost. By forming a coalition, every player in the coalition can obtain a gain through cooperation within the coalition. However, the gain is limited by a cooperation cost for forming the coalition, e.g., the negotiation cost or information exchange cost.

Given the player set and the coalition value, the coalition formation game is uniquely defined, and the outcome of the game is a set of coalitions, which is the optimal partitions of the player set. To obtain the optimal partitions, there are two possible approaches: centralized approach and distributed approach. For the centralized approach, the centralized controller needs to search over all the partitions of the player set to find the optimal partitions, which is NP-complete and impractical when the size of the player set is large [32]. For the distributed approach, the players will make their own decisions as to whether or not they join a coalition. One typical approach is to use the merge and split rules proposed in [33]. This approach starts with an initial partition and repeats alternatively the merge and split rule: 1) merge rule: merge any set of coalitions into a single coalition if the new coalition can provide larger total coalition values; and 2) split rule: split a coalition into smaller coalitions if the resulting smaller coalitions can provide larger total coalition values.

In Section IV, we will discuss in details how to use the coalition formation game to formulate the image denoising problem, where each pixel/block will be treated as a player

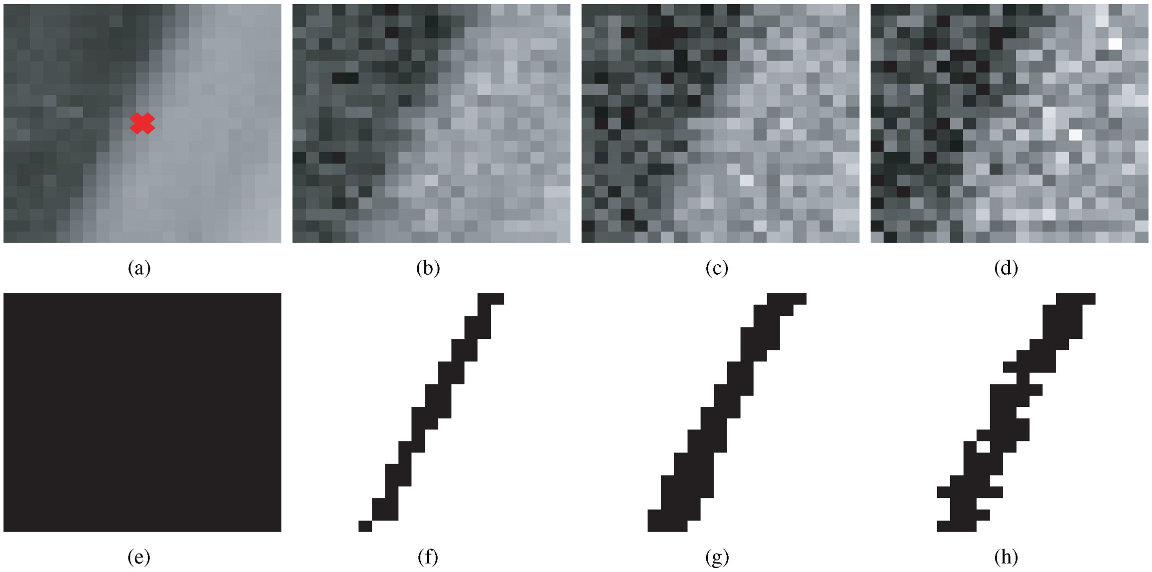

Fig. 1. Example of optimal candidate set with an edge region: (a) original image, (b) noisy image with $\sigma = 15$, (c) noisy image with $\sigma = 25$, (d) noisy image with $\sigma = 35$, (e) candidate set used by nonlocal, (f) ideally optimal candidate set of (b) when the original signal is available, (g) ideally optimal candidate set of (c) when the original signal is available, and (h) ideally optimal candidate set of (d) when the original signal is available.

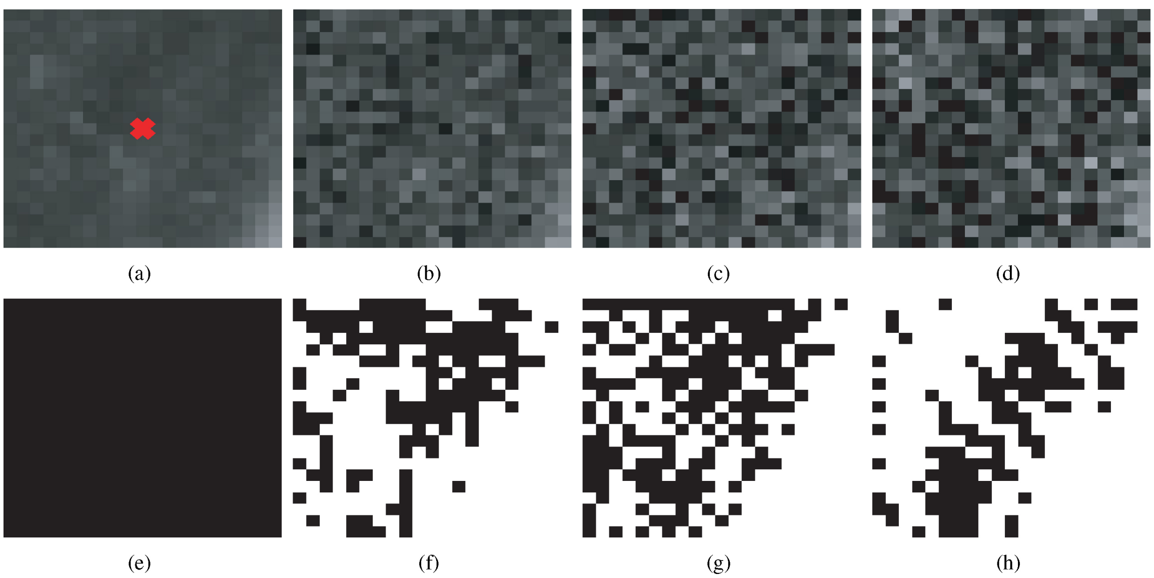

Fig. 2. Example of optimal candidate set with a smooth region: (a) original image, (b) noisy image with $\sigma = 15$, (c) noisy image with $\sigma = 25$, (d) noisy image with $\sigma = 35$, (e) candidate set used by nonlocal, (f) ideally optimal candidate set of (b) when the original signal is available, (g) ideally optimal candidate set of (c) when the original signal is available, and (h) ideally optimal candidate set of (d) when the original signal is available.

seeking to form coalitions to achieve optimal denoising performance.

III. Game Theoretical Problem Formulation

A. Parameter Selection

From (2), we can see that the reconstruction performance are determined by the selection of the weights $w_{\mathbf{k},\mathbf{l}}$ and the candidate set $S(\mathbf{k})$. For any given $S(\mathbf{k})$, the optimal weights $w^{\star}_{\mathbf{k},\mathbf{l}}(S(\mathbf{k}))$ are determined by the correlation between pixels $I(\mathbf{k})$ and $I(\mathbf{l})$, and should be chosen to minimize the difference between the estimation $\hat{I}(\mathbf{k})$ and the original pixel $I(\mathbf{k})$ as follows:

$$w^{\star}_{\mathbf{k},\mathbf{l}}(S(\mathbf{k})) = \arg\min_{w_{\mathbf{k},\mathbf{l}}} \left(\frac{\sum_{\mathbf{l}\in S(\mathbf{k})} w_{\mathbf{k},\mathbf{l}} I^n(\mathbf{l})}{\sum_{\mathbf{l}\in S(\mathbf{k})} w_{\mathbf{k},\mathbf{l}}} - I(\mathbf{k}) \right)^2. \quad (3)$$

Note that when the optimal weights in (3) are used, the selection of the candidate set $S(\mathbf{k})$ is trivial since the accuracy of the reconstruction improves as the candidate set $S(\mathbf{k})$ becomes larger. However, due to the absence of the original pixel $I(\mathbf{k})$, it is impossible for us to find the optimal weights using (3). One possible approximation is to use the similarity between the neighborhoods around $\mathbf{k}$ and $\mathbf{l}$ [26], which is defined as follows:

$$w_{\mathbf{k},\mathbf{l}} = \exp\left\{\frac{||\mathcal{P}(\mathcal{B}_{\mathbf{k}}) - \mathcal{P}(\mathcal{B}_{\mathbf{l}})||^2}{h^2}\right\} \quad (4)$$

where $\mathcal{B}_{\mathbf{k}}$ and $\mathcal{B}_{\mathbf{l}}$ are the predefined neighborhoods around $\mathbf{k}$ and $\mathbf{l}$, respectively, $\mathcal{P}(.)$ is a projection function such as principal component analysis (PCA), and h is the parameter related to the noise's variance.

Nevertheless, since the weights in (4) are not optimal, the selection of the candidate set $S(\mathbf{k})$ for the reconstruction becomes critically important. On one hand, if the size of the candidate set is too small, then the noise may not be effectively removed. On the other hand, if the size of the candidate set is too large, then the reconstruction may be overly-smooth. Moreover, according to (2) and (4), we can see that the reconstruction are also determined by the neighborhoods $\mathcal{B}_{\mathbf{k}}$ and $\mathcal{B}_{\mathbf{l}}$, the projection function $\mathcal{P}(.)$, and the parameter h. Obviously, all these parameters should be chosen in such a way that the difference between $\hat{I}(\mathbf{k})$ and $I(\mathbf{k})$ is minimized, i.e., the optimal parameters can be found by

$$\{S^\star(\mathbf{k}), \mathcal{B}^\star, \mathcal{P}^\star(.), h^\star\} = \arg \min_{S(\mathbf{k}),\mathcal{B},\mathcal{P}(.),h} |\hat{I}(\mathbf{k}) - I(\mathbf{k})|^2. \quad (5)$$

In general, the optimal parameters are content dependent, i.e., they may be different for different $\mathbf{k}$ and/or different noise variances. In Figs. 1 and 2, we show the structure of the optimal candidate set for two different scenarios: 1) the target pixel is centered within an edge region, and 2) the target pixel is centered within a smooth region. In these two figures, we fix $\mathcal{B}^\star$, $\mathcal{P}^\star(.)$, $h^\star$, and assume that the candidate set contains the pixels with the first m largest weights. For illustration purpose, we further assume that the original image is available for finding the optimal $m^\star$ in these two examples. In the following subsections, we will discuss how to find the optimal parameters using game theory under the scenario that the original image is not available. As shown in Figs. 1 and 2, (a) is the original image centered by the target pixel, which is denoted by red "x," (b)–(d) are the noisy images with σ being 15, 25, and 35, respectively. (e) is the candidate set using in [9], which is a pre-defined square window. (f)–(h) are the optimal candidate sets with optimal $m^\star$ for (b)–(d) respectively. Note that the black pixels in (f)–(h) stand for the pixels in the candidate set. From Figs. 1 and 2, we can see that for the scenario where the target pixel is centered within an edge region, the candidate set has an edge structure, while for the scenario where the target pixel is centered within a smooth region, the structure of the candidate set is unpredictable. Moreover, we can also see that with different noise variance, the candidate sets are quite different. Therefore, all the parameters in (2) including the candidate set $S(\mathbf{k})$ should not be predefined in a fixed way. Instead, the parameters should be chosen adaptively to minimize the difference between the estimate and the original signal.

B. Stein's Unbiased Risk Estimate (SURE)

Since $I(\mathbf{k})$ is unknown, the optimal parameters can not be explicitly computed using (5). Fortunately, we can first use the Stein's unbiased risk estimate (SURE) [24] to estimate the

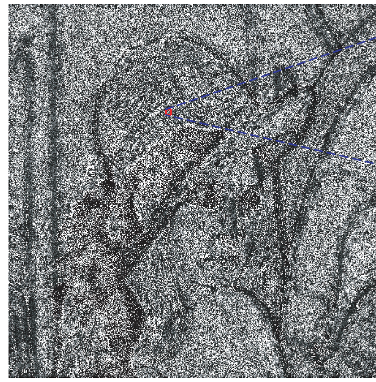

8	441	6	28	310	296	26	441
5	138	49	16	6	389	225	441
58	177	88	28	6	441	240	23
37	62	12	191	312	3	7	1
71	93	315	72	441	10	58	441
441	5	252	35	441	8	144	441
85	254	10	36	12	185	14	51
306	2	2	20	10	59	60	155

Fig. 3. Optimal size of the candidate set for *Lena* image when $\sigma = 10$.

true mean squared error (MSE) from the noisy observation and then use the estimated MSE to find the optimal parameters.

In Fig. 3, by fixing other parameters, we show the optimal size of the candidate set for *Lena* image when the standard deviation of the noise is $\sigma = 10$, where the intensity stands for the optimal size value. From Fig. 3, we can see that there are many pixels that have the similar optimal size value, which can be grouped together for finding the optimal size. For example, the pixels in the red circles have the optimal size value near 60 can be grouped together.

Suppose that the whole image is partitioned into M subsets $\Phi = \{\Phi_1, \Phi_2, ..., \Phi_M\}$, where each subset Φ_i contains a set of pixels that may not be physical neighboring but have the same optimal parameters, that is

$$\{S^\star(\mathbf{k}), \mathcal{B}^\star, \mathcal{P}^\star(.), h^\star\} = \arg \min_{S(\mathbf{k}),\mathcal{B},\mathcal{P}(.),h} \sum_{\mathbf{k}\in\Phi_i} |\hat{I}(\mathbf{k}) - I(\mathbf{k})|^2. \quad (7)$$

With the optimal parameters, the mean square error (MSE) for the subset Φ_i can be computed by

$$mse_i = \frac{1}{|\Phi_i|} \sum_{\mathbf{k}\in\Phi_i} |\hat{I}(\mathbf{k}|S^\star(\mathbf{k}), \mathcal{B}^\star, \mathcal{P}^\star(.), h^\star) - I(\mathbf{k})|^2 \quad (8)$$

and such a MSE can be approximated using SURE, according to Theorem 1, as follows:

$$SURE_i = \frac{1}{|\Phi_i|} \sum_{\mathbf{k}\in\Phi_i} |\hat{I}(\mathbf{k}|S^\star(\mathbf{k}), \mathcal{B}^\star, \mathcal{P}^\star(.), h^\star) - I^n(\mathbf{k})|^2 + \sigma^2 \left(\frac{2}{|\Phi_i|} \sum_{\mathbf{k}\in\Phi_i} \frac{\partial \hat{I}(\mathbf{k}|S^\star(\mathbf{k}), \mathcal{B}^\star, \mathcal{P}^\star(.), h^\star)}{\partial I^n(\mathbf{k})} - 1 \right) \quad (9)$$

where $\frac{\partial \hat{I}(\mathbf{k}|S^\star(\mathbf{k}),\mathcal{B}^\star,\mathcal{P}^\star(.),h^\star)}{\partial I^n(\mathbf{k})}$ can be found by (6) (shown at the top of page 5) with $\frac{\partial w_{\mathbf{k},\mathbf{l}}}{\partial I^n(\mathbf{k})}$ being determined by the projection function $\mathcal{P}^\star(.)$.

Theorem 1: The $SURE_i$ in (9) is an unbiased estimator of the true MSE mse_i in (8), that is

$$E[SURE_i] = E[mse_i]. \quad (10)$$

Proof: By substituting $I(\mathbf{k})$ with $I^n(\mathbf{k}) - n(\mathbf{k})$, we can

$$\frac{\partial \hat{I}(\mathbf{k}|S^\star(\mathbf{k}), \mathcal{B}^\star, \mathcal{P}^\star(.), h^\star)}{\partial I^n(\mathbf{k})} = \frac{1}{\sum_{\mathbf{l}\in S^\star(\mathbf{k})} w_{\mathbf{k},\mathbf{l}}} \left(\sum_{\mathbf{l}\in S^\star(\mathbf{k})} \frac{\partial w_{\mathbf{k},\mathbf{l}}}{\partial I^n(\mathbf{k})} I^n(\mathbf{l}) + 1 - \hat{I}(\mathbf{k}|S^\star(\mathbf{k}), \mathcal{B}^\star, \mathcal{P}^\star(.), h^\star) \sum_{\mathbf{l}\in S^\star(\mathbf{k})} \frac{\partial w_{\mathbf{k},\mathbf{l}}}{\partial I^n(\mathbf{k})} \right) \tag{6}$$

re-write $E[mse_i]$ as follows:

$$\begin{aligned} E[mse_i] &= E\left[\frac{1}{|\Phi_i|}\sum_{\mathbf{k}\in\Phi_i} |\hat{I}(\mathbf{k}|S^\star(\mathbf{k}), \mathcal{B}^\star, \mathcal{P}^\star(.), h^\star) - I(\mathbf{k})|^2\right] \\ &= E\left[\frac{1}{|\Phi_i|}\sum_{\mathbf{k}\in\Phi_i} \Big(|\hat{I}(\mathbf{k}|S^\star(\mathbf{k}), \mathcal{B}^\star, \mathcal{P}^\star(.), h^\star) - I^n(\mathbf{k})|^2 \right. \\ &\quad \left. + 2n(\mathbf{k})\hat{I}(\mathbf{k}|S^\star(\mathbf{k}), \mathcal{B}^\star, \mathcal{P}^\star(.), h^\star) - n(\mathbf{k})^2 \Big)\right] \\ &= \frac{1}{|\Phi_i|}\sum_{\mathbf{k}\in\Phi_i} E\left[|\hat{I}(\mathbf{k}|S^\star(\mathbf{k}), \mathcal{B}^\star, \mathcal{P}^\star(.), h^\star) - I^n(\mathbf{k})|^2\right] \\ &\quad + 2\frac{1}{|\Phi_i|}\sum_{\mathbf{k}\in\Phi_i} E\left[n(\mathbf{k})\hat{I}(\mathbf{k}|S^\star(\mathbf{k}), \mathcal{B}^\star, \mathcal{P}^\star(.), h^\star)\right] - \sigma^2. \end{aligned} \tag{11}$$

According to Stein's Lemma [24], we have

$$\begin{aligned} &E\left[n(\mathbf{k})\hat{I}(\mathbf{k}|S^\star(\mathbf{k}), \mathcal{B}^\star, \mathcal{P}^\star(.), h^\star)\right] \\ &= \sigma^2 E\left[\frac{\partial \hat{I}(\mathbf{k}|S^\star(\mathbf{k}), \mathcal{B}^\star, \mathcal{P}^\star(.), h^\star)}{\partial I^n(\mathbf{k})}\right]. \end{aligned} \tag{12}$$

Then, by substituting (12) back to (11), we have

$$\begin{aligned} E[mse_i] &= E\left[\frac{1}{|\Phi_i|}\sum_{\mathbf{k}\in\Phi_i} |\hat{I}(\mathbf{k}|S^\star(\mathbf{k}), \mathcal{B}^\star, \mathcal{P}^\star(.), h^\star) - I^n(\mathbf{k})|^2 \right. \\ &\quad \left. + \sigma^2\left(\frac{2}{|\Phi_i|}\sum_{\mathbf{k}\in\Phi_i} \frac{\partial \hat{I}(\mathbf{k}|S^\star(\mathbf{k}), \mathcal{B}^\star, \mathcal{P}^\star(.), h^\star)}{\partial I^n(\mathbf{k})} - 1\right)\right] \\ &= E[SURE_i]. \end{aligned}$$

■

C. Confidence and Distortion Tradeoff

1) *Confidence:* From Theorem 1, we can see that $SURE_i$ is an unbiased estimator of mse_i. However, there can be some mismatch between $SURE_i$ and mse_i for each realization (noise observation), i.e., $SURE_i$ is just an approximation of mse_i. To measure the accuracy of the approximation, let us define the confidence term, C, as the average difference between $SURE_i$ and mse_i over the whole image

$$C = \frac{1}{|\Phi|}\sum_{i=1}^{M} |\Phi_i| \times |mse_i - SURE_i|. \tag{13}$$

According to [24], the estimator $SURE_i$ becomes closer to mse_i as $|\Phi_i|$ increases, which means that the confidence term C in (13) decreases as $|\Phi_i|$ increases.

2) *Distortion:* With the partition $\Phi = \{\Phi_1, \Phi_2, ..., \Phi_M\}$ and the correspondingly optimal parameters, we can compute the mean square error for the whole image, D, as follows

$$D = \frac{1}{|\Phi|}\sum_{i=1}^{M} |\Phi_i| \times mse_i. \tag{14}$$

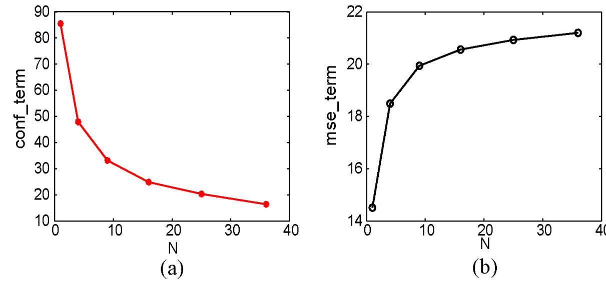

Fig. 4. Tradeoff between the confidence term C and the distortion term D. (a) Performance of C with different N. (b) Performance of D with different N.

According to the analysis in Section III-A, we group the pixels with similar optimal parameters together and assign a common group of optimal parameters to all pixels in subset Φ_i. In such a case, as $|\Phi_i|$ increases, the probability that the pixels in Φ_i have different true optimal parameters increases, which leads to the increase of mse_i. Therefore, the distortion term D in (14) increases as $|\Phi_i|$ increases.

3) *Confidence and Distortion Tradeoff:* From the above discussion, we can see that as $|\Phi_i|$ increases, the confidence term C decreases but the distortion term D increases. Therefore, there exists a tradeoff between C and D. To verify such a tradeoff, we conduct a simple experiment by setting $|\Phi_i| = N, \forall i$. As shown in Fig. 4, the confidence term C decrease as N increases while the distortion term D increases as N increases, which are consistent with our analysis.

D. Utility Function and Solution to the Game

From the previous subsections, we can see that given the partition $\Phi = \{\Phi_1, \Phi_2, ..., \Phi_M\}$, SURE can be used to approximate the true MSE to find the optimal parameters. However, how to find a good partition is not trivial since the number of the partition is not fixed and the size of each partition can vary. Due to the uncertainty of the number of the partition, the traditional segmentation and clustering methods may not work. To study the complex interactions among different pixels and the dynamic partition formation process, we propose to use the coalition formation game.

In this game theoretical formulation, every pixel is treated as a player, who tries to seek partners to form coalitions to achieve better reconstruction. By forming a coalition, every player in the coalition can obtain a gain of reducing the difference between the SURE and the true estimate, i.e., the confidence term in (13), while incurring a cost of increasing the minimum of the MSE. With this idea in mind, we define the utility for a coalition as

$$U(\Phi_i) = -|\Phi_i| \times SURE_i + g(|\Phi_i|, \sigma^2) \tag{15}$$

where the first term of the right hand side is the cost and the second term $g(|\Phi_i|, \sigma^2)$ is the gain.

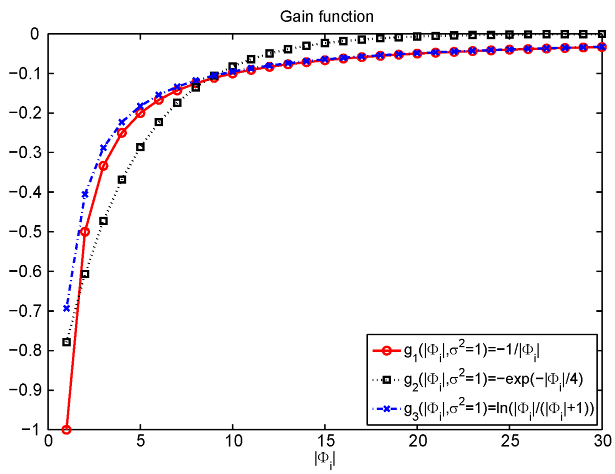

Fig. 5. Some possible gain functions.

The function $g(|\Phi_i|, \sigma^2)$ in (15) characterizes the gain of forming a coalition, which is the reduction of the difference between the SURE and the true estimate due to the increase of the coalition size. Therefore, $g(|\Phi_i|, \sigma^2)$ should satisfy the following properties.

1) $g(|\Phi_i|, \sigma^2)$ should be an increasing function in terms of $|\Phi_i|$ since the gain increases as the coalition size $|\Phi_i|$ increases, i.e., $\frac{\partial g(|\Phi_i|,\sigma^2)}{\partial |\Phi_i|} > 0$.
2) $g(|\Phi_i|, \sigma^2)$ should be a concave function in terms of $|\Phi_i|$ since a certain increase of the coalition size in the low $|\Phi_i|$ region should lead to a more significant gain than that in the high $|\Phi_i|$ region, i.e., $\frac{\partial^2 g(|\Phi_i|,\sigma^2)}{\partial |\Phi_i|^2} < 0$.
3) $g(|\Phi_i|, \sigma^2)$ should be a superadditive function since the gain of a large coalition should be no smaller than that of two sub coalitions, i.e., $g(|\Phi_i + \Phi_j|, \sigma^2) \geq g(|\Phi_i|, \sigma^2) + g(|\Phi_j|, \sigma^2)$.
4) $g(|\Phi_i|, \sigma^2)$ should be a decreasing function in terms of σ^2 since the gain decreases as noise variance σ^2 increases, i.e., $\frac{\partial g(|\Phi_i|,\sigma^2)}{\partial \sigma^2} < 0$.

There are many functions that can satisfy the above property. In the following, we list three possible functions:

$$g_1(|\Phi_i|, \sigma^2) = \lambda_1 \sigma^2 \left(\frac{-1}{|\Phi_i|} \right) \tag{16}$$

$$g_2(|\Phi_i|, \sigma^2) = \lambda_2 \sigma^2 \left[-\exp\left(\frac{-|\Phi_i|}{4} \right) \right] \tag{17}$$

$$g_3(|\Phi_i|, \sigma^2) = \lambda_3 \sigma^2 \left[\ln\left(\frac{|\Phi_i|}{|\Phi_i|+1} \right) \right] \tag{18}$$

where λ_1, λ_2, and λ_3 are fixed parameters.

In Fig. 5, we plot the three possible gain functions versus $|\Phi_i|$ by setting $\sigma^2 = 1$. We can see that all the three functions meet our requirements and are therefore valid gain functions. Moreover, we can see that all three functions behave similarly. Therefore, in this paper, we only evaluate the first gain function, i.e., $g(|\Phi_i|, \sigma^2)$ in (15) is set to be $g_1(|\Phi_i|, \sigma^2)$. Nevertheless, similar results can be obtained with the other two functions ($g_2(|\Phi_i|, \sigma^2)$ and $g_3(|\Phi_i|, \sigma^2)$) and any other functions with similar properties.

With the utility function in (15), we can see that as the size of the coalition increases, the members in the coalition can obtain gains from $g(|\Phi_i|, \sigma^2)$. However, the gains are limited by the a cost of forming the coalition, which is $-|\Phi_i| \times SURE_i$. The problem now is to find the optimal coalition structures based on the utility function in (15). One possible approach is to use the merge and split rules proposed in [33], where the authors prove that their algorithm will converge to a unique solution with arbitrary merge and split iterations. However, the computation complexity is still very large since all possible sub-partitions need to be evaluated during the split process. To make the problem traceable, in this paper, we propose a heuristic algorithm in solving the coalition formation game. The proposed heuristic algorithm starts with partitioning the image into blocks. Then, for each block, the proposed algorithm finds the coalition by selecting the neighborhoods that can give best average utility and derives the optimal parameters for the coalition. Finally, all the pixels in the block are denoised with the corresponding optimal parameters. The above procedures are repeated until all pixels are denoised. The proposed heuristic algorithm is distributive, and only locally neighboring information is required for finding the coalition. Moreover, since it is not an iterative algorithm, there is no convergence issue. Compared with the merge and split rules [33], the computation complexity is greatly reduced since the split process is avoided. From the experimental results shown in Section VI, we can see that the proposed heuristic algorithm performs quite well.

IV. Relation to the Traditional Approaches

In the traditional pixel-domain image denoising approaches, every pixel is denoised using (2) with the same parameters for the whole image. For example, a fixed-size square window centered by the target pixel **k** is chosen as the candidate set for the whole image in the nonlocal image denoising method [9]. Such kinds of approaches have a performance limitation due to the self-constrained use of same parameters for the whole image. As shown in Figs. 1 and 2, we can see that the parameters including the candidate set should be adaptively chosen for different pixels/blocks and/or noise variances. Moreover, we will show in the following analysis that the traditional methods such as the nonlocal method [9] and SURE-Nonlocal method [26] are actually special cases of the proposed game theoretic framework by choosing a utility function without a cost term

$$U(\Phi_i) = g(|\Phi_i|, \sigma^2). \tag{19}$$

According to the discussion in Section III-C, we know that a valid gain function $g(|\Phi_i|, \sigma^2)$ should be monotonically increasing, concave, and superadditive in terms of $|\Phi_i|$. In such a case, if the utility function only involves the gain function as in (19), then all pixels will form a grand coalition and use the same parameters. In such a case, it returns to the traditional approaches where the same parameters are used for all pixels. In this sense, we can say that the traditional approaches are special cases of the proposed game theoretic framework.

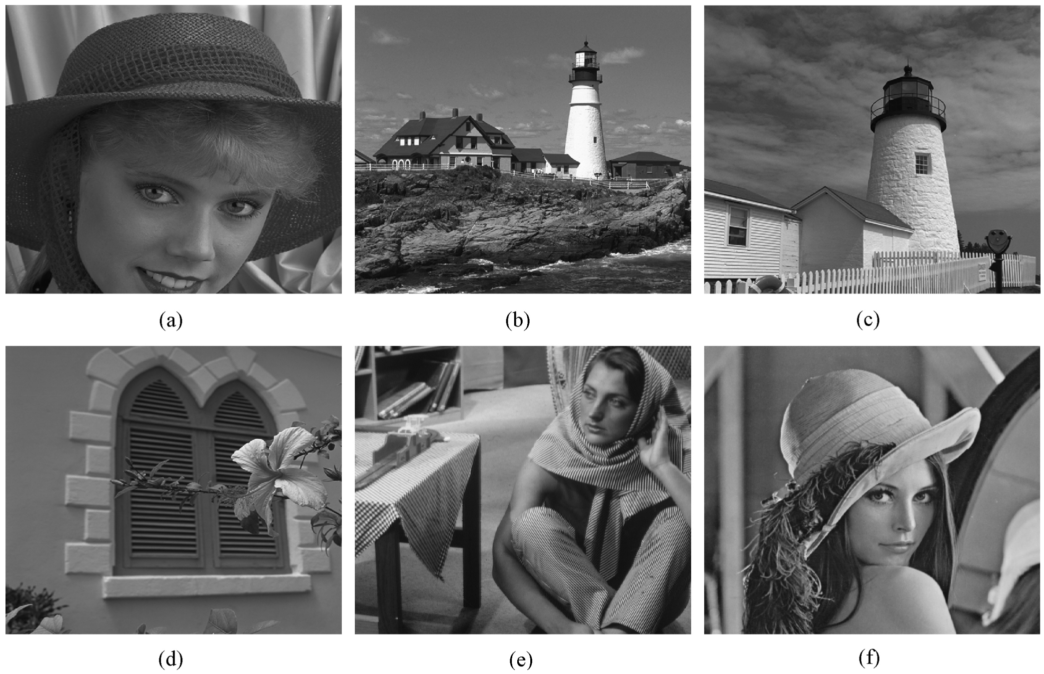

Fig. 6. Six 512x512 tested images: (a) image1. (b) image2. (c) image3. (d) image4. (e) *barbara*. (f) *lena*.

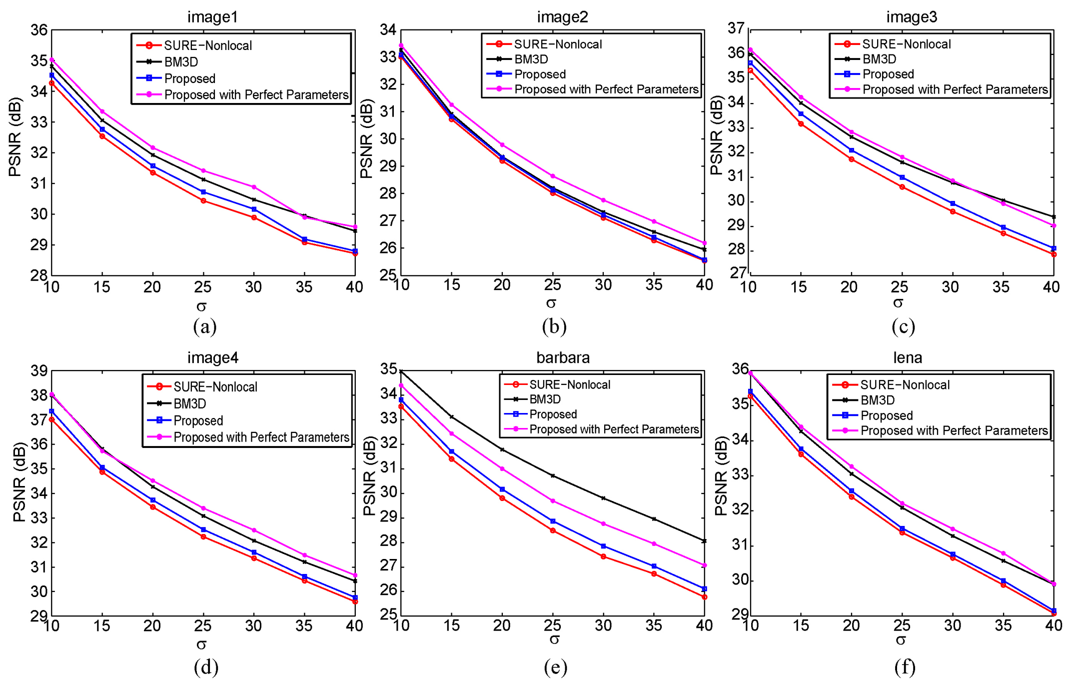

Fig. 7. PSNR comparison for different images: (a) image1. (b) image2. (c) image3. (d) image4. (e) *barbara*. (f) *lena*.

V. Experimental Results

We evaluate the proposed game theoretic image denoising approach by comparing it with the SURE-Nonlocal method [26] and BM3D method [19]. Six 512×512 images shown in Fig. 6: image1, image2, image3, image4, *Barbara* and *Lena*, are tested. The neighborhood $\mathcal{B}$ set is $\{3 \times 3, 5 \times 5, 7 \times 7, 9 \times 9\}$ and the candidate set is $\{5 \times 5, 7 \times 7, ..., 33 \times 33\}$. The dimensionality of projection $\mathcal{P}$ is set to be 6 and the parameter h^2 ranges from $0.7|\mathcal{B}|\sigma^2$ to $2|\mathcal{B}|\sigma^2$ with $|\mathcal{B}|$ being the size of the neighborhood.

We first evaluate the PSNR comparison versus the standard derivation of the noise. We compare the PSNR performance among four different approaches: SURE-Nonlocal [26], BM3D [19], the proposed game theoretic method denoted as "Proposed," and the "Proposed with Perfect Parameters" method where a genius is assumed to choose the optimal parameters. The results for different tested images at different noise levels are shown in Fig. 7. From Fig. 7, we can see that the proposed method always performs better than the SURE-Nonlocal method for all tested images at all different noise variances. The average gain of

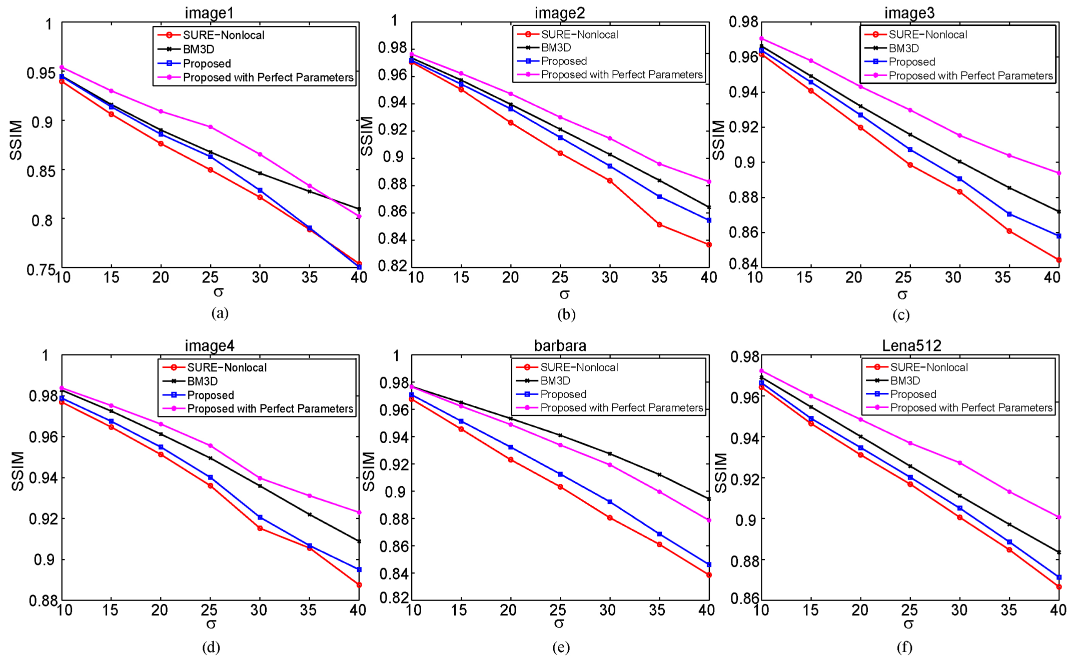

Fig. 8. SSIM comparison for different images: (a) image1. (b) image2. (c) image3. (d) image4. (e) *barbara*. (f) *lena*.

Fig. 9. Visual quality comparison for image1 with σ = 15. (a) Original image. (b) Noisy image. (c) Result generated by BM3D [19] (PSNR=33.05dB, SSIM=0.916). (d) Result generated by the SURE-Nonlocal [26] (PSNR=32.54dB, SSIM=0.9061). (e) Result generated by the proposed approach (PSNR=32.77dB, SSIM=0.9137). (f) Result generated by the proposed approach with perfect parameters (PSNR=33.34dB, SSIM=0.9299).

the proposed method over SURE-Nonlocal is 0.22dB with the maximal gain up to 0.43dB. While BM3D performs better than the proposed method, the proposed method with perfect parameters can achieve comparable or even better performance than BM3D, which shows the great potential of the proposed method, i.e., with a better heuristic coalition formation method, the proposed method may achieve comparable performance with BM3D. Moreover, we would like to emphasize that the proposed method is a pixel-domain method while BM3D is a transform-domain approach with multiple model aggregation. Furthermore, although the proposed method achieve worse performance than BM3D in terms of PSNR performance, it can achieve comparable performance in terms of visual quality, which will be shown later. We also evaluate the structural similarity (SSIM) [34] comparison and the results are shown in Fig. 8. We can see clearly that the proposed method outperforms the SURE-Nonlocal method and performs slightly worse than BM3D. However, with the perfect parameters, the proposed method can achieve much better SSIM performance than BM3D, which again shows the great potential of the proposed method.

(a) (b) (c)

(d) (e) (f)

Fig. 10. Visual quality comparison for image2 with σ = 25. (a) Original image. (b) Noisy image. (c) Result generated by BM3D [19] (PSNR=28.21dB, SSIM=0.9213). (d) Result generated by the SURE-Nonlocal [26] (PSNR=28.02dB, SSIM=0.9038). (e) Result generated by the proposed approach (PSNR=28.13dB, SSIM=0.9153). (f) Result generated by the proposed approach with perfect parameters (PSNR=28.64dB, SSIM=0.9302).

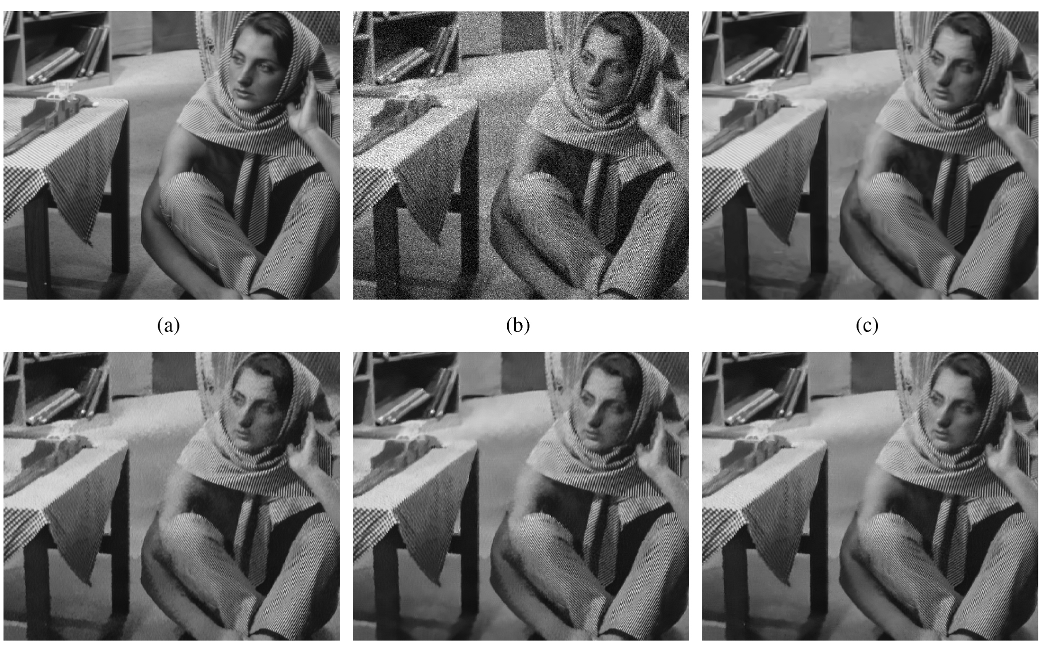

(a) (b) (c)

(d) (e) (f)

Fig. 11. Visual quality comparison for barbara with σ = 30. (a) Original image. (b) Noisy image. (c) Result generated by BM3D [19] (PSNR=29.80dB, SSIM=0.9274). (d) Result generated by the SURE-Nonlocal [26] (PSNR=27.43dB, SSIM=0.8805). (e) Result generated by the proposed approach (PSNR=27.86dB, SSIM=0.8923). (f) Result generated by the proposed approach with perfect parameters (PSNR=28.76dB, SSIM=0.9194).

(a) (b) (c) (d) (e) (f)

Fig. 12. Visual quality comparison for *lena* with σ = 35. (a) Original image. (b) Noisy image. (c) Result generated by BM3D [19] (PSNR=30.58dB, SSIM=0.8971). (d) Result generated by the SURE-Nonlocal [26] (PSNR=29.89dB, SSIM=0.8847). (e) Result generated by the proposed approach (PSNR=30.01dB, SSIM=0.8886). (f) Result generated by the proposed approach with perfect parameters (PSNR=30.79dB, SSIM=0.9131).

(a) (b) (c) (d) (e) (f)

Fig. 13. Visual quality comparison for image3 with σ = 20. (a) Original image. (b) Noisy image. (c) Result generated by BM3D [19] (PSNR=32.64dB, SSIM=0.9320). (d) Result generated by the SURE-Nonlocal [26] (PSNR=31.73dB, SSIM=0.9198). (e) Result generated by the proposed approach (PSNR=32.10dB, SSIM=0.9269). (f) Result generated by the proposed approach with perfect parameters (PSNR=32.84dB, SSIM=0.9431).

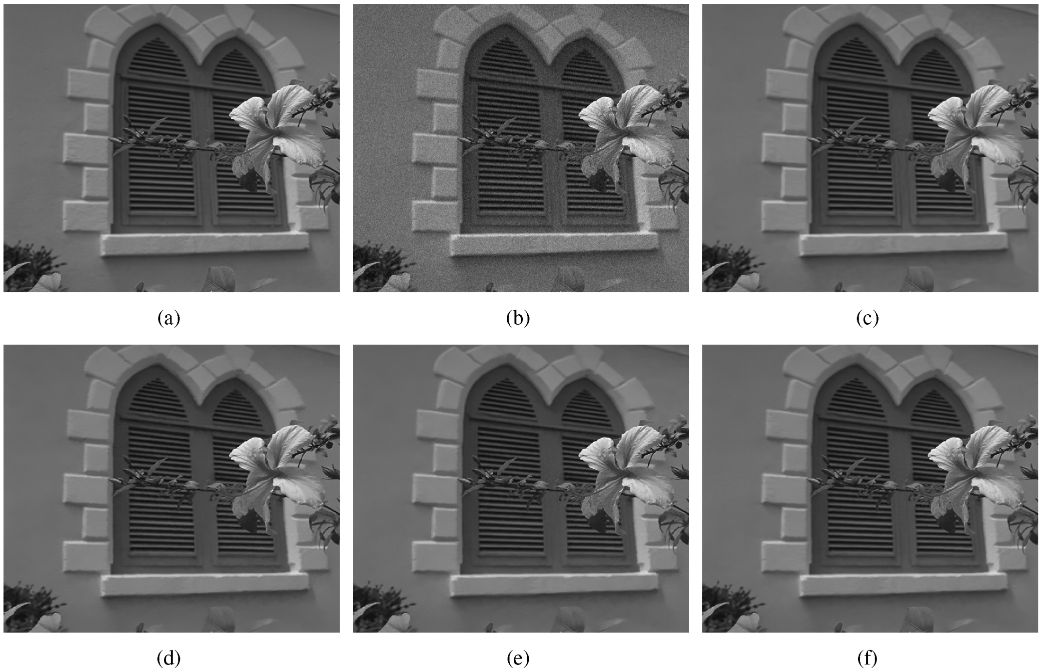

Fig. 14. Visual quality comparison for image4 with σ = 10. (a) Original image. (b) Noisy image. (c) Result generated by BM3D [19] (PSNR=38.00dB, SSIM=0.9827). (d) Result generated by the SURE-Nonlocal [26] (PSNR=37.01dB, SSIM=0.9769). (e) Result generated by the proposed approach (PSNR=37.35dB, SSIM=0.9788). (f) Result generated by the proposed approach with perfect parameters (PSNR=38.04dB, SSIM=0.9838).

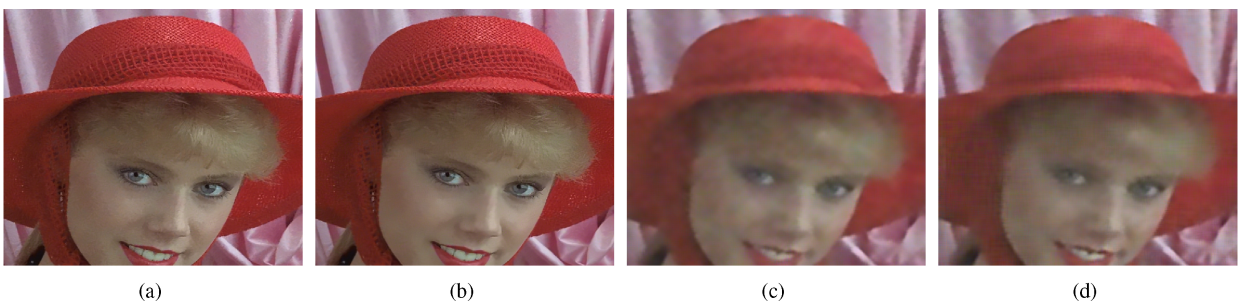

Fig. 15. Visual quality comparison for color version of image1. (a) Result generated by the SURE-Nonlocal with σ = 20[26] (PSNR=31.97 dB, SSIM=0.8946). (b) Result generated by the proposed approach with σ = 20(PSNR=32.20 dB, SSIM=0.8997). (c) Result generated by the SURE-Nonlocal with σ = 80[26] (PSNR=24.20 dB, SSIM=0.6731). (d) Result generated by the proposed approach with σ = 80(PSNR=24.20 dB, SSIM=0.6673).

Then, we evaluate the visual quality of the reconstructions.[2] In Fig. 9, we show the visual quality comparison for the image "image1." As shown in Fig. 9, (a) is the original image and (b) is the noisy image with σ = 15. The results generated by BM3D, SURE-Nonlocal, the proposed method and the proposed method with perfect parameters are shown in (c), (d), (e) and (f), respectively. The corresponding PSNR of the reconstructions are 33.05dB, 32.54dB, 32.77dB and 33.34dB, respectively. From Fig. 9, we can see that the result generated by the SURE-Nonlocal has a lot of visual artifacts such as the fake edge artifacts on the face region. This phenomenon is because the SURE-Nonlocal method chooses a common set of parameters for all pixels, i.e., a grand coalition is used. In such a case, a lot of pixels use non-optimal parameters for the reconstruction, which leads to the visual artifacts. With the proposed approach, every pixel/block (player) seeks parters to form coalition to determine the best parameters to perform denoising, which can adaptively choose the optimal parameters and avoid the visual artifacts. Moreover, although the proposed method achieves lower PSNR performance than BM3D, the visual quality performance of the proposed method is better than that of BM3D. From 9 (c), we can see that the result generated by BM3D has the contour artifact on the face region and over-smooth artifact on the left brim of the hat. Furthermore, when the perfect parameters are used, the visual quality performance of the proposed method can be further improved.

Fig. 10 shows the reconstructed results of "image2" at noise level σ = 25, while (a)–(e) are the original image, noisy image, the image reconstructed by BM3D, the image reconstructed by SURE-Nonlocal, the image reconstructed by the proposed method and the image reconstructed by the proposed method with perfect parameters, respectively. The PSNR of the reconstructed images are 28.21, 28.02, 28.13 and 28.64 dB, respectively. From Fig. 10, we can see that the visual quality of the

[2]All the experimental results shown in the paper can be downloaded on http://www.ece.umd.edu/~yan/imagedenoisinggames.zip

result generated by the proposed method is better than that of SURE-Nonlocal and BM3D, especially in the sky region above the house and the grass region below the house. The SURE-Nonlocal tends to produce fake edge artifact in the sky region while the BM3D tends to over-smooth the reconstruction in the grass region.

We also show the visual quality of the reconstructions of *barbara*, *lena*, "image3" and "image4" at different noise levels in Figs. 11, 12, 13, and 14, respectively. Similar to previous experiments, the proposed method can greatly reduce the noise and restore the image with better visual quality than SURE-Nonlocal and comparable (if not better than) visual quality with the BM3D. Due to the page limitation, we only show the results of one σ for each image in this paper. Similar results are observed for different $\sigma's$.

The proposed method can be also applied to the color images by performing denoising on RGB or YUV components. In Fig. 15, we show the visual quality comparison for color version of "image1." We can see that when the noise variance is not high, e.g. $\sigma = 20$, the proposed method can achieve better PSNR performance as well as better visual quality compared with SURE-Nonlocal. However, when the noise variance is high, e.g., $\sigma = 80$, our approach has little improvement. This is mainly because when the noise variance is high, more pixels are needed to have a reliable estimate of the true MSE. In such a case, pixels/blocks tend to form a big coalition, which leads to the performance similar to the SURE-Nonlocal method where a grand coalition is used.

VI. Conclusion

In this paper, we studied the tradeoff between the accuracy of the Stein's estimate and the minimum of the true MSE and formulated the image denoising problem as a coalition formation game. With the proposed game, every player (pixel/block) sought partners to form coalitions to obtain better decision for the optimal parameters selection and thus led to better denoising results. The experimental results showed that compared to SURE-Nonlocal, the proposed game theoretic approach achieved not only better PSNR performance but also better visual quality, while compared to BM3D, the proposed method had lower PSNR performance but comparable or even better visual quality. Moreover, the proposed method with perfect parameters further improved the performance significantly, which showed the great potential of the proposed method. Note that the proposed game is also applicable to other scenarios besides the pixel-domain approach as long as: 1) there exist some locally adaptive parameters to be estimated and 2) the estimation accuracy improves when more samples are involved in the estimate process. Furthermore, we showed that the traditional approaches using same parameters for the whole image were special cases of the game theoretic framework by choosing the utility function without a cost term.

References

[1] J. Woods and C. Radewan, "Kalman filtering in two dimensions," *IEEE Trans. Inform. Theory*, vol. 23, no. 4, pp. 473–482, Jul. 1977.

[2] F. Jin, P. Fieguth, L. Winger, and E. Jernigan, "Adaptive Wiener filtering of noisy images and image sequences," in *Proc. IEEE Int. Conf. Image Process.*, 2003, pp. 349–352.

[3] S. M. Smith and J. M. Brady, "Susan: A new approach to low level image processing," *Int. J. Comput. Vision*, vol. 23, no. 1, pp. 45–78, May 1997.

[4] M. Elad, "On the origin of the bilateral filter and ways to improve it," *IEEE Trans. Inform. Theory*, vol. 10, no. 10, pp. 1141–1151, Oct. 2002.

[5] C. Tomasi and R. Manduchi, "Bilateral filtering for gray and color images," in *Proc. 6th Int. Conf. Comput. Vision*, 1998, pp. 839–846.

[6] T. Chan and J. Shen, "Image processing and analysis: variational, PDE, wavelet, and stochastic methods," in *Proc. SIAM*, 2005.

[7] G. Gilboa, N. Sochen, and Y. Y. Zeevi, "Image enhancement and denoising by complex diffusion processes," *IEEE Trans. Pattern Anal. Machine Intell.*, vol. 26, no. 8, pp. 1020–1036, Aug. 2004.

[8] G. Gilboa, N. Sochen, and Y. Y. Zeevi, "Variational denoising of partly-textured images by spatially varying constraints," *IEEE Trans. Image Process.*, vol. 15, no. 8, pp. 2281–2289, Aug. 2006.

[9] A. Buades, B. Coll, and J. M. Morel, "A review of image denoising algorithms, with a new one," *SIAM Multiscale Model. Simulat.*, vol. 4, no. 2, pp. 490–530, Jul. 2005.

[10] A. Buades, B. Coll, and J. M. Morel, "The staircasing effect in neighborhood filters and its solution," *IEEE Trans. Image Process.*, vol. 15, no. 6, pp. 1499–1505, Jun. 2006.

[11] C. Kervrann and J. Boulanger, "Optimal spatial adaptation for patch-based image denoising," *IEEE Trans. Image Process.*, vol. 15, no. 10, pp. 2866–2878, Oct. 2006.

[12] C. Kervrann and J. Boulanger, "Local adaptivity to variable smoothness for exemplar-based image regularization and representation," *Int. J. Comput. Vision*, vol. 79, no. 1, pp. 45–69, Aug. 2008.

[13] D. L. Donoho, "De-noising by soft-thresholding," *IEEE Trans. Inform. Theory*, vol. 41, no. 3, pp. 613–627, May 1995.

[14] A. Pizurica, W. Philips, I. Lemahieu, and M. Acheroy, "A joint inter and intrascale statistical model for bayesian wavelet based image denoising," *IEEE Trans. Image Process.*, vol. 11, no. 5, pp. 545–557, May 2002.

[15] O. Guleryuz, "Weighted averaging for denoising with overcomplete dictionaries," *IEEE Trans. Image Process.*, vol. 16, no. 12, pp. 3020–3034, Dec. 2007.

[16] Y. Hel-Or and D. Shaked, "A discriminative approach for wavelet shrinkage denoising," *IEEE Trans. Image Process.*, vol. 17, no. 4, pp. 443–457, Apr. 2008.

[17] F. Abramovich and Y. Benjamini, "Adaptive thresholding of wavelet coefficients," *Comput. Stat. Data Anal.*, vol. 22, pp. 351–361, Aug. 1996.

[18] M. Elad, "Why shrinkage is still relevant for redundant representations?" *IEEE Trans. Inform. Theory*, vol. 52, no. 12, pp. 5559–5569, Dec. 2006.

[19] K. Dabov, A. Foi, V. Katkovnik, and K. Egiazarian, "Image denoising by sparse 3-D transform-domain collaborative filtering," *IEEE Trans. Image Process.*, vol. 16, no. 8, pp. 2080–2095, Aug. 2007.

[20] J. Mairal, F. Bach, J. Ponce, G. Sapiro, and A. Zisserman, "Non-local sparse models for image restoration," in *Proc. ICCV*, 2009.

[21] W. Dong, L. Zhang, G. Shi, and X. Li, "Nonlocally centralized sparse representation for image restoration," *IEEE Trans. Image Process.*, vol. 22, no. 4, pp. 1620–1630, Apr. 2013.

[22] A. Levin and B. Nadler, "Natural image denoising: optimality and inherent bounds," in *Proc. CVPR*, Sep. 2011.

[23] A. Levin, B. Nadler, and F. D. W. T. Freeman, "Patch complexity, finite pixel correlations and optimal denoising," in *Proc. ECCV*, 2012.

[24] C. Stein, "Estimation of the mean of a multivariate normal distribution," *Ann. Statist.*, vol. 9, no. 6, pp. 1135–1151, Jan. 1981.

[25] D. V. D. Ville and M. Kocher, "Sure-based non-local means," *IEEE Signal Process. Lett.*, vol. 16, no. 11, pp. 973–976, Nov. 2009.

[26] D. V. D. Ville and M. Kocher, "Nonlocal means with dimensionality reduction and sure-based parameter selection," *IEEE Trans. Image Process.*, vol. 20, no. 9, pp. 2683–2690, Sep. 2011.

[27] D. L. Donoho and I. M. Johnstone, "Adapting to unknown smoothness via wavelet shrinkage," *J. Amer. Statist. Assoc.*, vol. 90, no. 432, pp. 1200–1224, Dec. 1995.

[28] A. Benazza-Benyahia and J.-C. Pesquet, "Building robust wavelet estimators for multicomponent images using stein's principle," *IEEE Trans. Image Process.*, vol. 14, no. 11, pp. 1814–1830, Nov. 2005.

[29] F. Luisier, T. Blu, and M. Unser, "A new sure approach to image denoising: Interscale orthonormal wavelet thresholding," *IEEE Trans. Image Process.*, vol. 16, no. 3, pp. 593–606, Mar. 2007.

[30] S. Ramani, T. Blu, and M. Unser, "Monte-Carlo sure: A black-box optimization of regularization parameters for general denoising algorithms," *IEEE Trans. Image Process.*, vol. 17, no. 9, pp. 1540–1554, Sep. 2008.
[31] Y. Chen and K. J. R. Liu, "A game theoretical approach for image denoising," in *Proc. IEEE ICIP*, 2010.
[32] D. Ray, *A Game-Theoretic Perspective on Coalition Formation*. Oxford, U.K.: Oxford Univ. Press, 2007.
[33] K. R. Apt and A. Witzel, "A generic approach to coalition formation," in *Proc. Int. Workshop COMSOC*, 2006.
[34] Z. Wang, A. C. Bovik, H. R. Sheikh, and E. P. Simoncelli, "Image quality assessment: From error visibility to structural similarity," *IEEE Trans. Image Process.*, vol. 13, no. 4, pp. 600–612, Apr. 2004.

Yan Chen (S'06–M'11) received the Bachelor's degree from the University of Science and Technology of China, Beijing, China, in 2004, the M.Phil. degree from the Hong Kong University of Science and Technology, Hong Kong, in 2007, and the Ph.D. degree from the University of Maryland, College Park, MD, USA, in 2011.

He is currently a Research Associate with the Department of Electrical and Computer Engineering, University of Maryland. His current research interests include social learning and networking, smart grids, cloud computing, crowdsourcing, network economics, multimedia signal processing, and communication.

Dr. Chen was a recipient of the University of Maryland Future Faculty Fellowship in 2010, the Chinese Government Award for outstanding students abroad in 2011, the University of Maryland ECE Distinguished Dissertation Fellowship Honorable Mention in 2011. He was a finalist of the A. James Clark School of Engineering Dean's Doctoral Research Award in 2011.

K. J. Ray Liu (F'03) was a Distinguished Scholar-Teacher with the University of Maryland, College Park, MD, USA, in 2007, where he is currently the Christine Kim Eminent Professor of Information Technology. He leads the Maryland Signals and Information Group conducting research encompassing broad areas of signal processing and communications with a recent focus on cooperative communications, cognitive networking, social learning and networks, and information forensics and security.

Dr. Liu is the recipient of numerous honors and awards, including the IEEE Signal Processing Society Technical Achievement Award and Distinguished Lecturer Award. He also received various teaching and research recognitions from the University of Maryland, including the University-Level Invention of the Year Award, and the Poole and Kent Senior Faculty Teaching Award and Outstanding Faculty Research Award, both from the A. James Clark School of Engineering. He is an ISI highly-cited author and a fellow of AAAS. He is President of the IEEE Signal Processing Society where he has served as the Vice President of Publications and on the Board of Governor. He was the Editor-in-Chief of *IEEE Signal Processing Magazine* and the founding Editor-in-Chief of the *EURASIP Journal on Advances in Signal Processing*.